

HOST-MICROBE INTERACTIONS

A dynamic mouse peptidome landscape reveals probiotic modulation of the gut-brain axis

Pei Zhang^{1,2*}, Xiaoli Wu^{3*}, Shan Liang^{3,4*}, Xianfeng Shao^{1,5*}, Qianqian Wang¹, Ruibing Chen⁵, Weimin Zhu¹, Chen Shao^{1†}, Feng Jin^{3†}, Chenxi Jia^{1‡}Copyright © 2020
The Authors, some
rights reserved;
exclusive licensee
American Association
for the Advancement
of Science. No claim
to original U.S.
Government Works

Certain probiotics have beneficial effects on the function of the central nervous system through modulation of the gut-brain axis. Here, we describe a dynamic landscape of the peptidome across multiple brain regions, modulated by oral administration of different probiotic species over various times. The spatiotemporal and strain-specific changes of the brain peptidome correlated with the composition of the gut microbiome. The hippocampus exhibited the most sensitive response to probiotic treatment. The administration of heat-killed probiotics altered the hippocampus peptidome but did not substantially change the gut microbiome. We developed a literature-mining algorithm to link the neuropeptides altered by probiotics with potential functional roles. We validated the probiotic-regulated role of corticotropin-releasing hormone by monitoring the hypothalamic-pituitary-adrenal axis, the prenatal stress-induced hyperactivity of which was attenuated by probiotics treatment. Our findings provide evidence for modulation of the brain peptidome by probiotics and provide a resource for further studies of the gut-brain axis and probiotic therapies.

INTRODUCTION

The human intestines contain a complex community of microorganisms that are increasingly recognized as an important contributor to the regulation of the physiology, metabolism, and immunity of the host (1, 2). Emerging evidence suggests that the gut microbiota is associated with many neurological processes, including neurotransmission, neurogenesis, neuroinflammation, and neuroendocrine signaling, which further influences the host's psychology and social behavior (1–4). Dysbiosis of the gut microbiome possibly contributes to many behavioral and mental diseases, such as autism spectrum disorders (5), Alzheimer's disease (6), Parkinson's disease (7), depression (8, 9), and anxiety (10, 11). Brain and gut communicate bidirectionally through the gut-brain axis by three major communication pathways: the vagus nerve, the immune response, and the microbial metabolites (8). Although important roles of the gut-brain axis have been identified, the underlying mechanisms are still unclear.

Probiotics are live microorganisms that offer health benefits to the host (12). Many previous studies in rodent models suggest that probiotics administration can relieve some anxiety, depression, and autism-like behaviors through the gut-brain axis (12). Bravo *et al.* (13) reported that chronic treatment of healthy mice with *Lactobacillus rhamnosus* reduced anxiety-related behaviors and also induced region-dependent changes in transcripts encoding the metabotropic γ -aminobutyric acid receptor GABA_{B1b}, and a mouse strain effect was observed in a follow-up study (14). Hsiao *et al.* (15) demonstrated that ingestion of *Bacteroides fragilis* ameliorated abnormalities in

gut permeability and autism-related behavior in mice. Buffington *et al.* (16) found that *Lactobacillus reuteri* restored oxytocin production in the hypothalamus and corrected the social deficits of offspring in a mouse model of maternal diet-induced obesity. Liang *et al.* (17) showed that treatment of rats with *Lactobacillus helveticus* NS8 improved chronic stress-induced depression and cognitive dysfunction. In addition to these findings from rodent models, a clinical trial showed that subchronic administration of a probiotic formulation containing *L. helveticus* R0052 and *Bifidobacterium longum* R0175 alleviated psychological distress (11). Although many reports have indicated the beneficial consequences of probiotics as well as connections between microbiome, gut, and brain, it is still challenging to elucidate the underlying mechanisms, largely because of lack of in-depth molecular knowledge about this complex system.

Neuropeptides and peptide hormones are diverse classes of biological modulators. They are highly enriched in the central nervous system (CNS) and involved in most physiological and psychological processes, including reproduction, feeding, energy homeostasis, pain, memory, mood, anxiety, reward pathways, arousal, and sleep-wake cycles (18–25). Several reports have indicated that neuropeptides are involved in gut-brain communication (26, 27). If the gut microbiome can modulate the expression and secretion of peptides in the CNS, the downstream physiological processes and behavior of the hosts will be modulated or influenced (26). The changes can either benefit the fitness of the hosts or cause neurological disorders. Given the importance of the regulatory roles of brain peptides and previous findings in the brain-gut axis, we ask (i) whether the administration of probiotics can alter the brain peptidome and (ii) whether the brain peptidome and the gut microbiome are correlated.

Here, using a mass spectrometry (MS)-based peptidomics approach, we describe a dynamic landscape wherein the brain peptidome was influenced by probiotics administration and pinpoint the regulatory signature of peptidome changes. We found that remodeling of the brain peptidome by probiotics treatment exhibited spatiotemporal and probiotics strain-specific patterns, which were highly correlated with the composition of the gut microbiome. Collectively, these data open an avenue to investigate these signaling molecules

¹State Key Laboratory of Proteomics, Beijing Proteome Research Center, Beijing Institute of Lifeomics, National Center for Protein Sciences (The PHOENIX Center, Beijing), Beijing 102206, China. ²School of Life Sciences, Hebei University, Hebei Province, Baoding 071002, China. ³Key Laboratory of Mental Health, Institute of Psychology, Chinese Academy of Sciences, Beijing 100101, China. ⁴Key Laboratory of Microbial Physiological and Metabolic Engineering, Institute of Microbiology, Chinese Academy of Sciences, Beijing 100101, China. ⁵Department of Genetics, School of Basic Medical Sciences, Tianjin Medical University, Tianjin 300070, China. *These authors contribute equally to this work. †Corresponding author. Email: cja@mail.ncpsb.org (C.J.); jinffeng@psych.ac.cn (F.J.); shaochen@mail.ncpsb.org (C.S.) ‡Lead contact.

in the gut-brain axis by using high-throughput techniques and are a rich resource for the neuroscience and microbiology communities.

RESULTS

One-hour peptidomics enables accurate and rapid analysis of brain peptides

To systematically investigate the effects of gut microbiota on brain peptides, we subjected seven groups of naturally colonized adult male mice to four different 1-month treatment regimens and three different 2-month treatment regimens (Fig. 1A). The 1-month treatment regimens included mice fed plain water or water mixed with the probiotics *L. helveticus* NS8 (17), heat-killed NS8, or *Lactobacillus fermentum* NS9 (28), hereafter referred to as C, NS8, NS8h, or NS9 treatment, respectively. The 2-month treatment regimens included animals given only plain water (CC), water with NS8 for 1 month followed by plain water for 1 month (NS8C), or water with NS8 for 2 months (NS8NS8). After animals were euthanized, endogenous peptides across four brain regions (hypothalamus, hippocampus, striatum, and pituitary) were analyzed by MS-based peptidomics, and the gut microbiomes were assessed by 16S ribosomal RNA (rRNA) sequencing (Fig. 1A). This experimental design separates the effects of treatment into several variable factors, including different probiotic strains, treatment time, and brain regions as well as live versus heat-killed probiotics.

Extremely low concentrations of endogenous peptides, high dynamic range of peptide abundance, and relatively large sample cohorts are major challenges for peptidome analysis. To overcome these challenges, we established a “1-hour peptidomics” workflow (Fig. 1B) with the capability to identify 2598 modification-specific peptides (a peptide contains specific types and sites of modifications) from the tiny mouse hypothalamus by single-run liquid chromatography-tandem MS (LC-MS/MS), including neuropeptides, peptide hormones,

and other endogenous peptides. The high quality of quantitative results using this method was demonstrated by mass accuracy, confidence score, reproducibility, and quantitative accuracy, among other factors [figs. S1 (A to E) and S2 (A and B)].

The 1-hour peptidomics approach was further benchmarked across multiple brain regions by the analysis of 12 mice from the dataset of C group, resulting in the identification of 2290, 1162, 1262, and 4620 modification-specific peptides from hypothalamus, hippocampus, striatum, and pituitary, respectively (Fig. 2A and data file S1). The pituitary gland contained the largest number of endogenous peptides with the highest dynamic range of abundance. Our results also show that some peptides displayed highly dynamic expression in different regions. For example, neuropeptide Y (NPY) ranked among the top 30 in abundance in hippocampus, hypothalamus, and striatum but ranked as low in abundance in the pituitary. We also plotted the cumulative abundance of peptides in the hypothalamus (Fig. 2B) and summarized the families represented in the top 75% of these peptides (Fig. 2C and table S1). There were six peptides that accounted for the first 25% of the total accumulative intensity, and three of these have well-studied functions, namely, little-SAAS, big-LEN, and somatostatin-28(1-12) (Fig. 2B). This finding highlights the challenge of brain peptide analytics due to the high dynamic range of peptide abundance. Collectively, the 1-hour peptidomics approach enabled high-throughput analysis of brain peptides and generated a brain region-resolvable resource with 6315 identified modification-specific peptides in total.

Probiotics treatment induces remodeling of the brain peptidome

To evaluate the effect of probiotics treatment, we performed label-free quantitative analysis on the peptidomics data between the NS8 and C groups. After treatment, 366 of 2230 quantifiable brain peptides

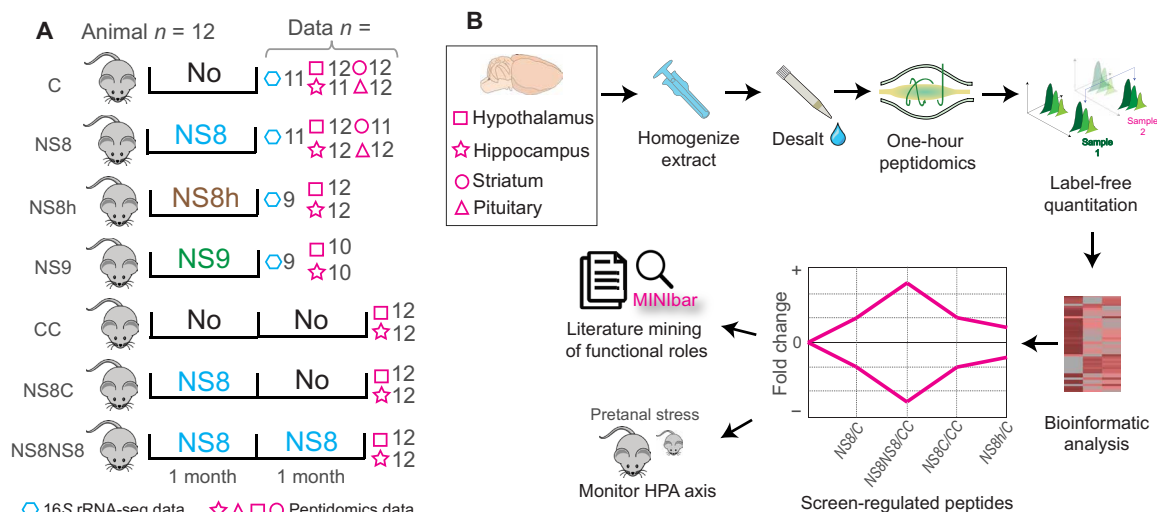


Fig. 1. Experimental design and integrated peptidomics workflow. (A) Seven groups of mice ($n = 12$ animals in each group) were differentially treated with plain water (C), *L. helveticus* NS8 (NS8), *L. fermentum* NS9 (NS9), or heat-killed NS8 (NS8h) for 1 or 2 months as shown. After treatment, gut microbiome composition (16S rRNA sequencing) and brain peptidomics data were generated for each group. The n value for each omics dataset is indicated next to the symbol for that dataset. For data analysis, all the data in each group were combined. The n value for data in some omics sets is less than the number of animals in each experiment ($n = 12$) because of failed sample preparation or data acquisition. C, 1-month control; NS8, 1-month NS8 treatment; NS8h, 1-month heat-killed NS8 treatment; NS9, 1-month NS9 treatment; CC, 2-month control; NS8C, 1-month NS8 treatment and 1-month nontreatment; NS8NS8, 2-month NS8 treatment. (B) Integrated workflow for in-depth analysis of brain peptidomes.

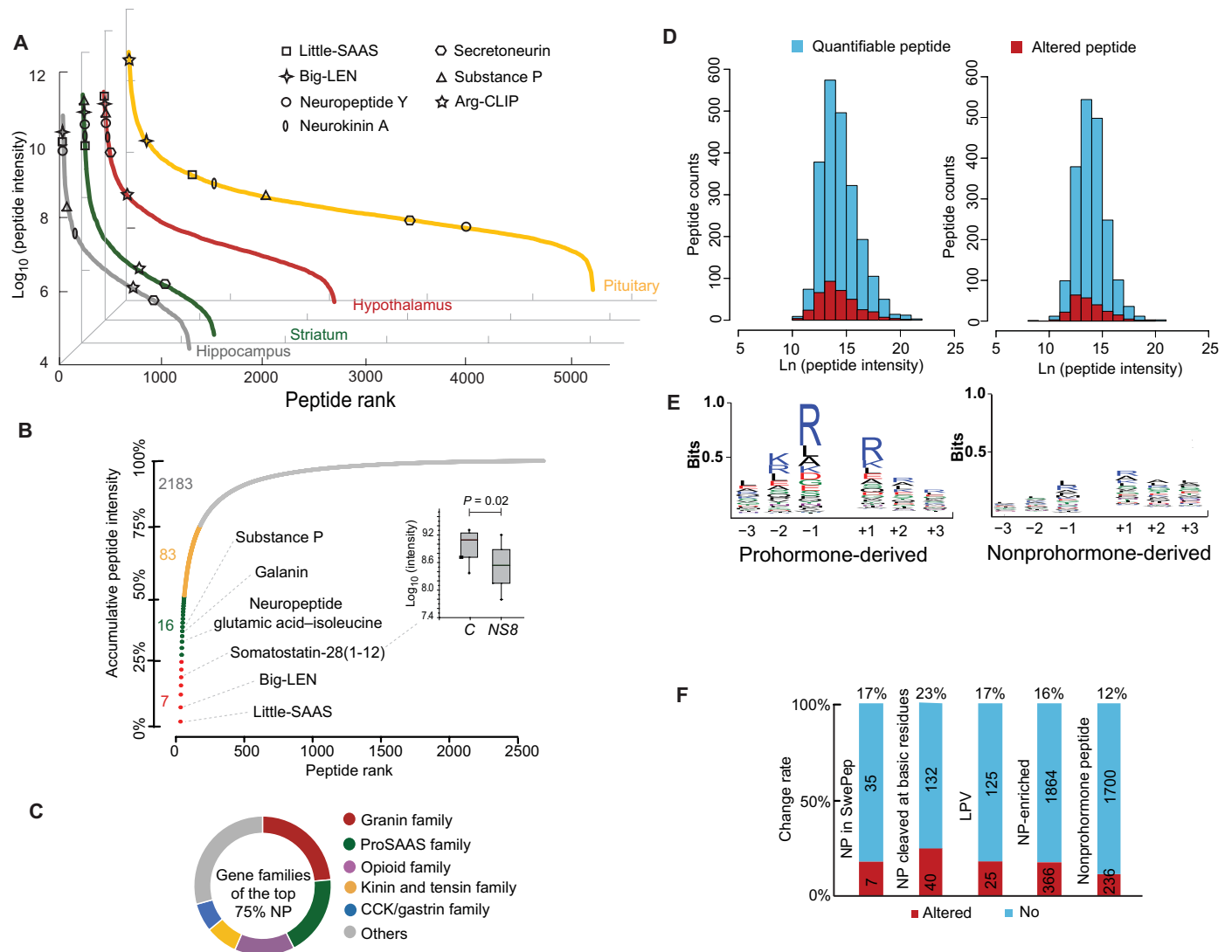


Fig. 2. Benchmarking the 1-hour peptidomics approach and peptidome changes upon probiotics administration. (A) Dynamic range of brain peptides based on peptide intensities across four brain regions in control animals given plain water for 1 month (group C). Values for some peptides are noted, and the complete list of identified peptides is in data file S1. (B) Cumulative abundance of peptides in the hypothalamus of group C from the highest to the lowest abundance. The box plot inset shows the change in somatostatin-28(1-12) abundance induced by probiotics treatment. (C) Families to which the top 75% of neuropeptides (by accumulative intensity) in the hypothalamus of group C animals belong. (D) Histogram illustrating the quantifiable and significantly altered peptides in hypothalamus after 1-month of NS8 treatment compared to 1 month of no treatment (NS8/C) including the prohormone-derived (left) and nonprohormone-derived peptides (right). Unique sequences and abundance data are shown in data file S2. (E) Logo plot illustrating the motifs present in the terminal regions flanking peptides corresponding to the quantifiable peptides in (D) and data file S2. (F) Rate of NS8-induced change of neuropeptide-derived peptides compared to control. CCK, cholecystokinin; NP, neuropeptide; LPV, longest peptide variants. Significance of altered peptides was calculated by a two-tailed *t* test ($P < 0.05$).

(unique sequences) were found to have significant changes in abundance (data file S2), and the peptide intensity and count information were further clustered into a histogram (Fig. 2D, left). Some of the C- and N-terminal linear sequence motifs of the quantifiable peptides displayed a feature characteristic of neuropeptides, the dibasic cleavage site KR or the monobasic cleavage site R (Fig. 2E, left), which are consistent with the cleavage rules of the enzymatic processing of neuropeptides (29). In addition to neuropeptides derived from prohormones, there are thousands of endogenous peptides derived from nonprohormone proteins, which were simultaneously acquired in the LC-MS/MS data. To compare the response sensitivities

of neuropeptides and other endogenous peptides on probiotics treatment, we constructed a customized database based on UniProt mouse protein entries by removing the prohormone proteins and then conducted quantitative analysis using the LC-MS/MS data against this database. We obtained a set of nonprohormone peptides without enriched motifs (Fig. 2E, right, and data file S2) that was similar to a previous report on rat brain peptides (30). The histograms of peptide intensity and count information (Fig. 2D) show that the prohormone-derived peptide group had a higher rate of change in response to probiotic treatment than the nonprohormone-derived peptide group. This result indicates that neuropeptides acting as

important signaling molecules are more sensitive than nonprohormone peptides in response to probiotics treatments. Furthermore, we calculated the percentages of altered peptides due to probiotic treatment on three types of biological molecules, including (i) peptides in the SwePep database (31), (ii) the longest peptide variants (LPV) (30), and (iii) the neuropeptides produced at the cleavage site of basic residues (K/R in positions -1, +1, and +2) (29). These three types of biomolecules exhibited more neuropeptide-enriched features, and their rates of change were much higher than those of nonprohormone peptides (Fig. 2F). These results reveal that the probiotics treatment caused significant changes of neuropeptides and that the sensitivity of the response to treatment depended on the type of regulatory molecule.

Gut microbiome assessment reveals potential interaction with the brain peptidome

To discover the possible cause of brain peptide change through the gut-brain axis, we investigated the intestinal microbiome by analyzing the 16S rRNA datasets of groups C, NS8, and NS8h. For all groups, we obtained typical mouse microbiomes dominated by the phyla of Bacteroidetes and Firmicutes (fig. S3A). Although there was no significant intergroup difference by analysis of α diversity (fig. S3B), the principal coordinates analysis (PCoA) of β diversity indicated that the NS8 group differed more from the C and NS8h groups than the C and NS8h groups differed from one another (Fig. 3A, left). The NS8h group did not show statistically significant change in the gut microbiome compared to the C group. Next, we carried out principal components analysis (PCA) of the peptidome datasets from the hypothalamus and hippocampus (Fig. 3A, middle and right). In the hypothalamus, the change trend of the peptidome was observed as similar as that of the microbiome. Only the live NS8 treatment caused change of the brain peptidome, but the heat-killed NS8 treatment did not. Also, a brain region-specific effect was observed. In the PCA plot of hippocampus peptides, both of NS8 and NS8h groups were separated from the C group, indicating that treatment by heat-killed and live NS8 altered the hippocampus peptidome.

Four of the 115 annotated bacterial genera, belonging to the Lachnospiraceae and Ruminococcaceae families, were significantly altered by NS8 treatment (Fig. 3B). Previous reports showed that change of these two families occurs in multiple sclerosis (32), depression (33), and autism (34). Subsequently, we chose the four significantly altered bacterial genera, [*Eubacterium*] *xylanophilum* group, *Anaerotruncus*, *Ruminiclostridium* 5, and *Ruminococcaceae* UCG-013, to perform Spearman's rank correlation analysis with peptidome datasets across all samples (Fig. 3C, and data file S3 illustrate representative correlated peptides in hypothalamus). Vasoactive intestinal peptide (VIP) showed distinct correlation with *Anaerotruncus* (Fig. 3D). VIP is a 28-amino acid peptide that binds to class II heterotrimeric guanine nucleotide-binding protein-coupled receptors, playing an important role in the regulation of energy metabolism and circadian rhythm (35). *Anaerotruncus* is a bacterial genus belonging to the family Ruminococcaceae, which is also associated with energy metabolism. These results indicate possible regulatory connections between these bacterial genera and brain peptides through the gut-brain axis.

We observed that the treatment with live NS8 caused remarkable, correlated changes in the gut microbiome and hypothalamus peptidome (Fig. 3, A and B). This suggests that change of the microbiome composition is a possible pathway through which probiotics modulate brain peptides. To investigate the peptides associated with microbi-

ome change, we clustered those exclusively altered in the NS8 group (Fig. 3E and data file S4) and then grouped them into neuropeptide families (Fig. 3F). Granin, opioid, proSAAS, somatostatin (SMS), and F&Y amide families ranked at the top, suggesting potential functional responses of these groups of peptides to the changes in gut microbiota. In addition, the NS8h group showed a different pattern of peptide abundances from those of the C group (Fig. 3E).

Brain peptide changes upon probiotics treatment display region-specific patterns

To provide a bird's-eye view of brain peptide expression profile upon probiotics treatment, we aggregated peptidomics information by the family to which neuropeptide belongs (36) and further clustered them into a circular peptide map across four brain regions (Fig. 4A and data file S5). Peptides in the pituitary gland were dominated by the granin and opioid families, both of which were less prevalent in the other three brain regions. By calculating the percentage of the altered peptides in each family (Fig. 4B), the cocaine- and amphetamine-regulated transcript family in hypothalamus showed a change rate of 33%.

To perform a comparative analysis of the response to probiotics treatment across brain regions, we evaluated two quantifiable values of brain peptides: change rate (ratio of altered to quantifiable peptide number) and fold change. The quantitative peptidomics data of the NS8 treatment group compared to that of the C group (NS8/C) of the four brain regions were aggregated into histograms showing peptide count versus intensity (Fig. 4C). The fold changes of increased or decreased brain peptides were further summarized into boxplots (Fig. 4C). The peptides in hippocampus showed the highest change rate at 33% and also the highest amount of increase, indicating the most sensitive response among the four regions under investigation. In contrast, the change rate of peptides in striatum was minimal, and the fold changes of the decreased peptides were the smallest. To some extent, the NS8 treatment suppressed the expression of some peptides in the striatum.

Next, we investigated the colocalization and coregulation of brain peptides across multiple regions. The peptidomics data of NS8/C were summarized into a multipanel, region-resolved bar graph (Fig. 4D and data file S6). Seventy-three percent of identified peptides were exclusively expressed in a single region, and almost 99% of the peptides that increased in abundance and 96% of the peptides that decreased in abundance displayed single region-specific distribution. Subsequently, we performed Spearman's rank correlation analysis between brain peptides and the change in gut bacterial genera, across different brain regions using the datasets of the C and NS8 groups. Representative peptides correlated with the four bacterial genera, including neuropeptides with functions in appetite regulation (Fig. 4, E and F), including the anorexigenic peptides α -melanocyte-stimulating hormone (α -MSH), β -MSH, neuromedin-B, and somatostatin-28(1-12), and the orexigenic peptides NPY and orexin (37). In addition, VIP and neuromedin-B displayed similar correlation pattern in two brain regions. The correlation between gut bacteria and brain peptides suggests possible modulatory relationships.

Multiple factors drive remodeling of the hypothalamus peptidome

To generate a global view of brain peptide change in the seven experimental groups (Fig. 1A), we processed hypothalamus peptidomics data by PCA and plotted the centric values of each group in a

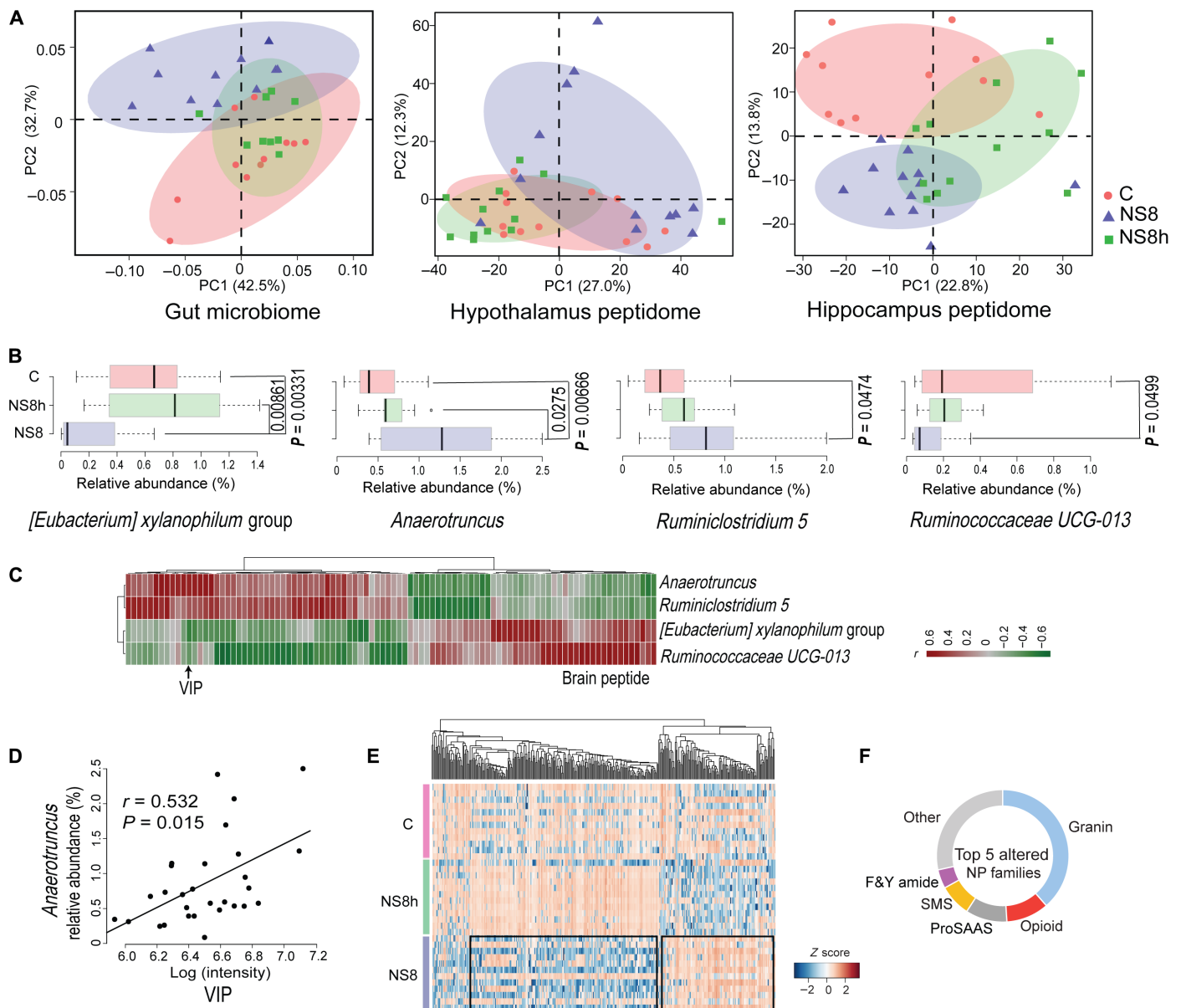


Fig. 3. Correlation between changes in the brain peptidome and gut microbiome upon 1-month treatment with the probiotic NS8 and heat-killed NS8. (A) PCoA plot of gut microbiome and PCA plots of the hypothalamus and hippocampus peptidomes after 1 month of treatment with live (NS8) or heat-killed (NS8h) NS8 compared to control animals (C). (B) Relative abundance of four bacterial genera in groups C, NS8, and NS8h. Two-tailed t test. (C) Heatmap showing the matrix of Spearman's correlation coefficient (r) of significantly altered bacterial genera and representative brain peptides in hypothalamus. $r < -0.5$ or $r > 0.5$ for at least one of the four bacterial genera. Details are available in data file S3. (D) Scatter plot showing the relationship between the abundance of vasoactive intestinal peptide (VIP) against the relative abundance of *Anaerotruncus* in the gut microbiome. (E) Hierarchical clustering of changes in the hypothalamus peptidome C, NS8h, and NS8 treatment groups. One-way analysis of variance (ANOVA), $P < 0.05$. The peptides exclusively altered in the NS8 group as compared to the C and NS8h groups are boxed, and complete data is included in data file S4. (F) Neuropeptide families of the hypothalamus peptidome that were exclusively altered in the NS8 group.

ternary diagram (Fig. 5A). The group CC was clearly separated from the C group, suggesting an effect of age that is independent of probiotic treatment. The 1-month treatment group NS8 was separated from the 1-month control group C along a different direction, and then the 2-month treatment group NS8NS8 was further separated from NS8 because of the combined effects of age and NS8 treatment. In addition, the NS9 and NS8h groups separated from group C in different directions by the effects of different probiotics strain

and live versus heat-killed bacteria, respectively. It should be noted that we only addressed the major effects. These results vividly illustrate the dynamic landscape of peptidome remodeling under various treatment conditions, which also raises questions about (i) whether the peptide change by probiotics treatment was time dependent; (ii) the extent of the effect of age on peptide change of adult mice; and (iii) whether differences between strains of probiotics result in different phenotypes of peptide change.

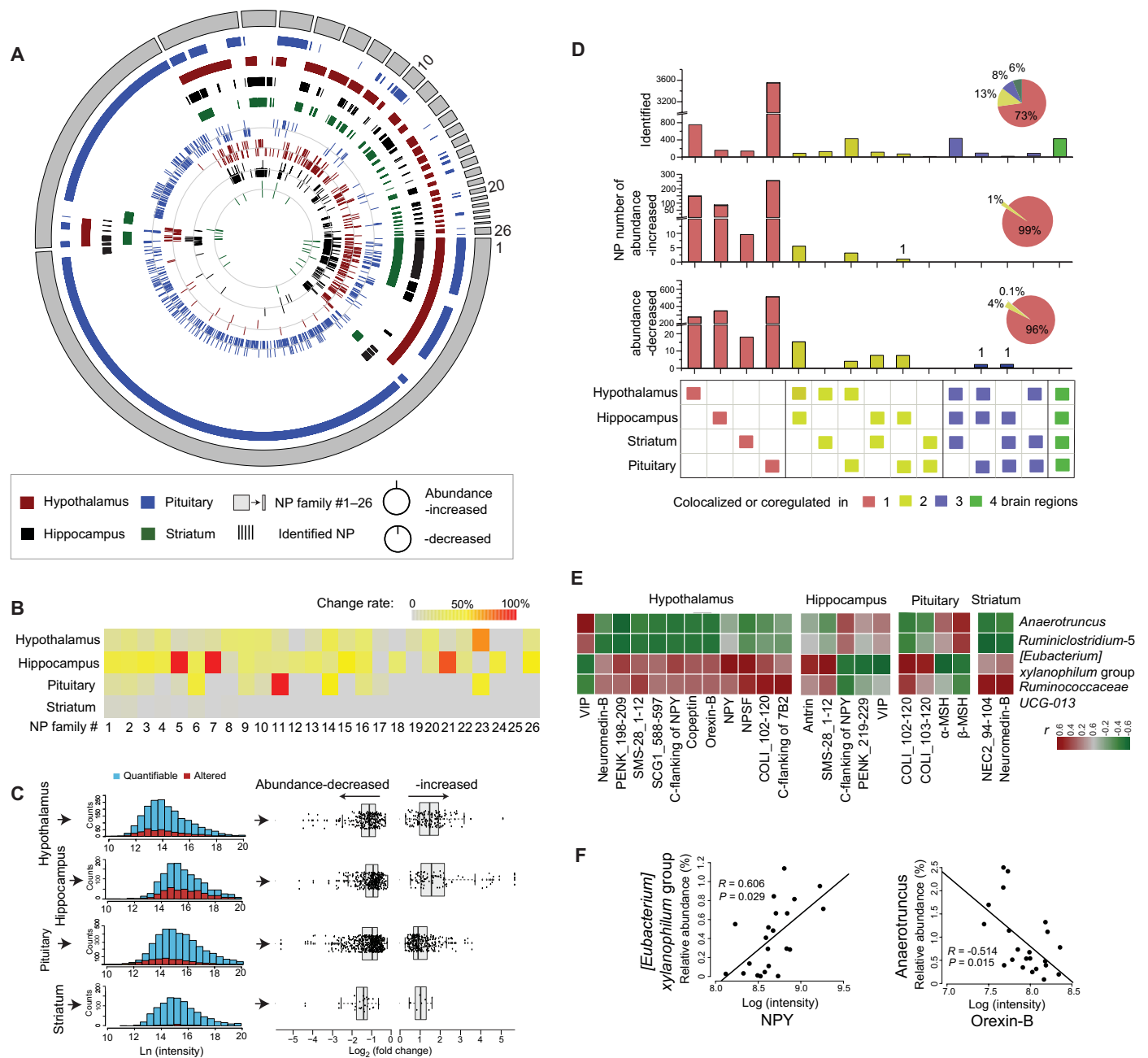
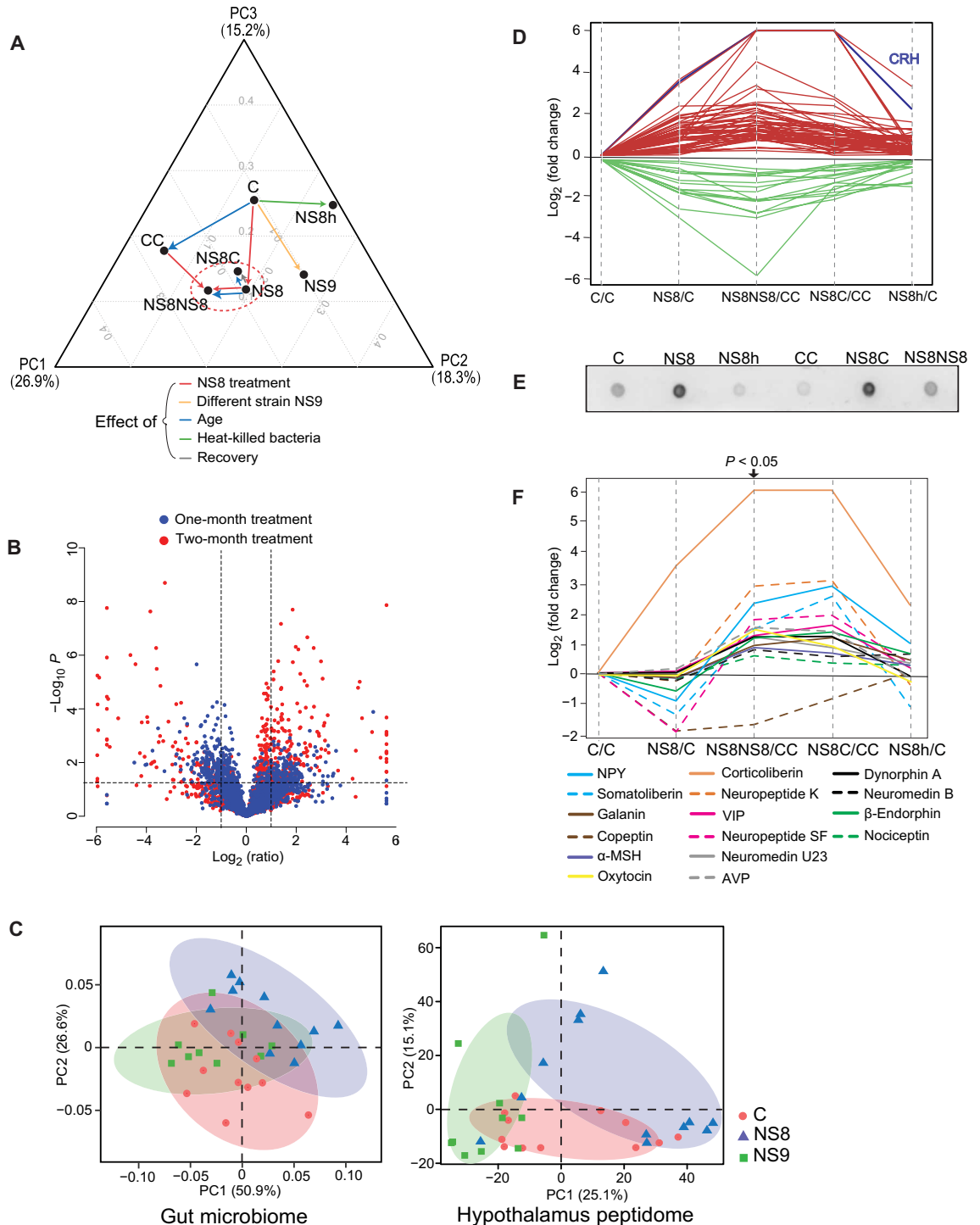


Fig. 4. Regional brain distribution and change of peptides in NS8-treated versus control animals. (A) Circular brain peptidome maps depict the qualitative, quantitative, and region-specific information in the peptidomes from control (group C) animals (details in data file S5). The outer ring indicates the neuropeptide families; the middle four rings are qualitative information of brain peptides in the four regions of the brain; the inner four rings are quantitative information for each of the four brain regions. The 26 neuropeptide families are listed in table S1. (B) Heatmap shows the change rate (altered/quantifiable peptides in a family) of brain peptide families in NS8-treated mice compared to control mice. (C) Histograms illustrate the quantifiable brain peptides that were altered in the four brain regions in NS8-treated mice compared to group C. Box plots show the fold change of the altered brain peptides (modification-specific peptides). (D) Bar graphs show the number of peptides that were identified, increased, or decreased in each brain region. Subsets of peptides that were present in multiple regions (colocalized) or showed similar changes in abundance in multiple regions (colocalization) are noted in the matrix below the graphs. The pie charts summarize the percentage of brain peptides that were coregulated in one, two, three, or all four brain regions. The details are shown in data file S6. (E) Heatmap shows the matrix of Spearman's correlation coefficient (r) of significantly altered bacterial genera and representative brain peptides across four brain regions. $r < -0.5$ or $r > 0.5$ for at least one of the four bacterial genera. (F) Scatter plots show the relationships between the abundances of neuropeptide Y (NPY) and orexin-B and the *[Eubacterium] xylanophilum* group and *Anaerotruncus* in the gut microbiome. The data were processed from quantitative data of NS8-treated versus control (NS8/C) in four brain regions. Significance of altered peptides was calculated by a two-tailed t test ($P < 0.05$), and peptides that increased or decreased in abundance were determined by mean differences.

Fig. 5. Changes in hypothalamus peptides across treatment conditions.

(A) Ternary PCA plot of the brain peptidome changes across the seven experimental groups C, NS8, NS8h, NS9, CC, NS8C, and NS8NS8. The colored arrows indicate treatment groups through which pairwise comparisons can identify changes specific to probiotic treatment, different probiotic strains, the 1-month age difference between animals, live versus heat-killed probiotic, and recovery from 1-month treatment with live NS8. (B) Volcano plots of altered brain peptides for 1- and 2-month treatment with NS8 compared to water-only controls (NS8/C and NS8NS8/CC). Two-tailed *t* test, *P* < 0.05. (C) PCoA plot of gut microbiome and PCA plot of hypothalamus peptidome for groups C, NS8, and NS9. (D) Screening curve showing putative probiotics-altered peptides that increased (red) or decreased (green) with NS8 treatment compared to control. CRH is highlighted in blue (data file S7, first sheet). (E) Dot blot validation of CRH abundance under the six indicated conditions. (F) Changes in the abundances of representative neuropeptides after 1-month (NS8) and 2-month (NS8NS8) NS8 treatment regimens relative to (C) the control groups as indicated (data file S7, second sheet). Peptides were selected by significance of a two-tailed *t* test for NS8NS8/CC, *P* < 0.05. AVP, arginine vasopressin; α -MSH, α -melanocyte-stimulating hormone.



To answer the first question, the peptidomic datasets of NS8/C and NS8NS8/CC were plotted into a two-layer volcano graph (Fig. 5B). The 2-month treatment results showed more remarkable changes than those of the 1-month treatment groups, indicating that the probiotics-induced change of the peptidome depended on the duration of treatment. To answer the second question, we performed differential analysis on the C and CC groups of peptidomics data.

The 1-month age difference between the adult mice at the end points of each experiment was responsible for a 29% of change rate (fig. S4), which is much higher than the 16% change rate resulting from NS8 treatment (Fig. 2F). This result indicates that animal development and age is a non-negligible factor in the effect of probiotics treatment on brain peptide changes. To answer the third question, we performed PCoA analysis of the microbiome and PCA analysis of the peptidome

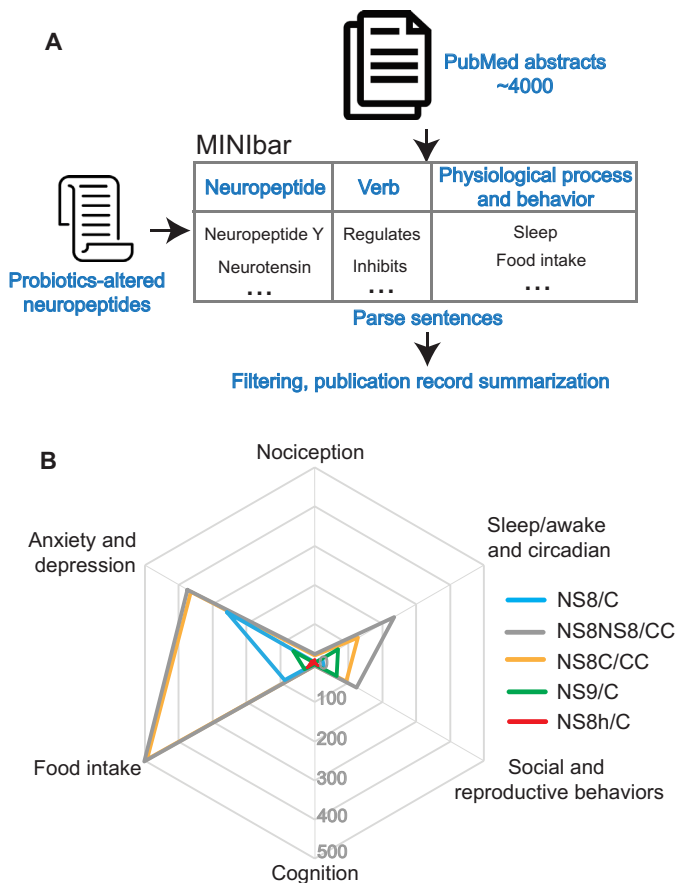


Fig. 6. The MINibar algorithm for text mining of behaviors related to specific neuropeptides in published abstracts. (A) Schematic showing how PubMed abstracts were mined to identify physiological processes and behaviors regulated by specific neuropeptides altered by probiotic treatment. (B) Radar diagram showing possible connections between probiotic treatments and behaviors predicted from publication mining. The five probiotic treatment conditions are linked with the six behaviors on the basis of numbers of publications reporting regulatory roles of neuropeptides on behaviors. Details are shown in data file S9.

of groups C, NS8, and NS9 (Fig. 5C). *L. helveticus* NS8 and *L. fermentum* NS9 are different species of *Lactobacillus* and exhibit distinct beneficial consequences mediated by distinct metabolic mechanisms (17, 28, 38). From the PCoA analysis of the gut microbiome data (Fig. 5C), we found that the NS9 treatment caused a much smaller change in the gut microbiome than did NS8 treatment. A similar effect was observed in PCA analysis of the hypothalamus peptidome. Subsequently, we carried out hierarchical clustering on the peptidomics data, which illustrates the peptide changes with the same and opposite trends by the treatments resulting from the strain-specific effect (fig. S5).

Probiotics-altered brain peptides show similar patterns of change

To narrow down the candidates of probiotics-altered brain peptides, we selected the peptides that changed in certain patterns under different treatment conditions. We hypothesized that a peptide altered by probiotics treatment would follow one of the trends shown in the peptide screening plot (Fig. 1B) and that the heat-killed probiotics

would be less effective than the live ones. For peptides that exhibited probiotics-dependent increase during the first month of treatment, the abundance would continue to increase during the second month of treatment and decrease during the second month of plain water only (Fig. 1B). Similarly, there should be a mirror trend for the peptides that exhibited a probiotics-dependent decrease in abundance during the first month of treatment—continuing to decrease in the second month of treatment and increasing during the subsequent month of plain water only. It should be noted that peptides could show a different trend in change due to probiotics treatment, such as an increase or decrease during the first month of treatment that remained unchanged after an additional month on plain water without continuing to change in abundance or reverse its change in abundance.

By using this screening strategy, we obtained 71 peptide candidates that followed the trends defined in the peptide screening plot (Figs. 1B and 5D and data file S7) in hypothalamus, including an increase in the well-studied neuropeptide corticotropin-releasing hormone (CRH) (Fig. 5, D and E), which is at the top of hypothalamus-pituitary-adrenal (HPA) axis. This increase in CRH might be induced by immune responses to the probiotics treatment (39). In addition to the peptides that followed the rules of clustering we established (Fig. 5D), many neuropeptides with important reported functions exhibited change only after the second month of NS8 treatment (Fig. 5F and data file S7), including oxytocin. Previously, Buffington *et al.* (16) found that *L. reuteri* reversed social deficits in the offspring of mice born to mothers on high-fat diet and proposed a model that *L. reuteri* improved social behavior by increasing oxytocin production and related functions. The dynamic variation of these functional molecules in our dataset suggests that chronic probiotics treatment might alter physiological processes and behaviors.

Literature mining reveals the functional roles of probiotics-altered neuropeptides

We constructed an algorithmic strategy called MINibar (Mining neuropeptide and related behavior) to mine PubMed for the functional roles and behaviors of neuropeptides altered in abundance by probiotics treatment (Fig. 6A). Five treatment conditions with altered neuropeptides were aligned with possible related physiological processes and behaviors by the numbers of publications supporting each association (Fig. 6B). For example, the 2-month NS8 treatment identified changes in 12 neuropeptides that are highly associated with anxiety and depression, as evidenced by 374 publications (Fig. 6B). This result is consistent with a previous report that NS8 improves stress-induced anxiety and depression-like behavior (17). In addition, food intake, social and reproductive behaviors, and sleep-wake and circadian cycles were also associated with the neuropeptides altered by probiotics treatment (Fig. 6B). These literature-based results provide evidence of association of NS8-altered peptides with phenotypic behaviors and also suggest potential applications for NS8.

NS8 treatment attenuates the increases in CRH and adrenocorticotrophic hormone induced by prenatal stress

To explore the possible functional consequences of probiotics-induced increases in CRH (Fig. 5, D and E), we investigated the effect of probiotics on prenatal stress-induced increases in CRH and adrenocorticotrophic hormone (ACTH), key elements of the HPA axis. Exposure to prenatal stress causes a hyperreactive response in the HPA axis in mice (40). Clinical studies have reported that the exposure of women to valproic acid (VPA) during pregnancy increases

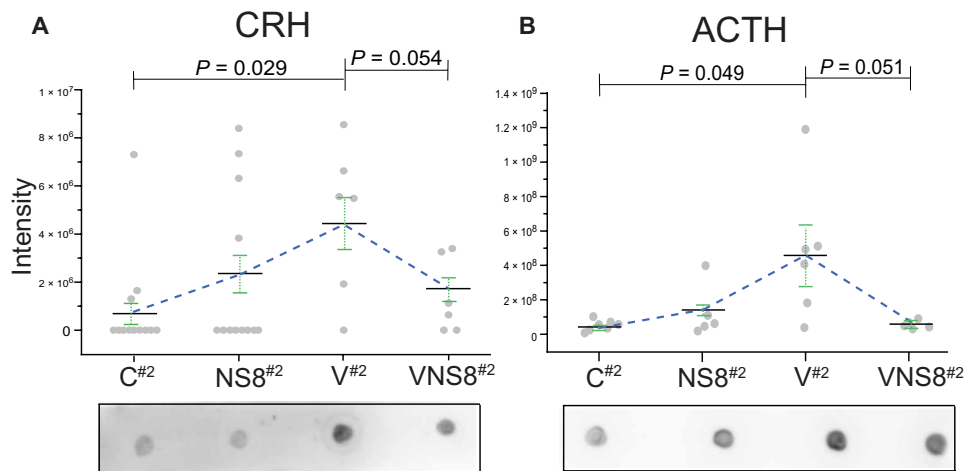


Fig. 7. Monitoring the brain peptide change of HPA axis upon prenatal stress and NS8 treatment. (A) Column scatter plot shows peptidomic intensities of CRH in the hypothalamus of control (C^{#2}, $n = 12$) and NS8-treated (NS8^{#2}, $n = 12$) offspring of untreated mothers and in the hypothalamus of control (V^{#2}, $n = 6$) and NS8-treated (VNS8^{#2}, $n = 6$) offspring of VPA-treated mothers. Below the graph, dot blots for CRH in peptides extracted from the hypothalamus of the indicated mice are shown. Blots are representative of independent experiments with samples from three different mice. (B) Column scatter plot shows peptidomic intensities of ACTH in the pituitary of control (C^{#2}, $n = 7$) and NS8-treated (NS8^{#2}, $n = 5$) offspring of untreated mothers and in the hypothalamus of control (V^{#2}, $n = 6$) and NS8-treated (VNS8^{#2}, $n = 5$) offspring of VPA-treated mothers. Below the graph, dot blots for ACTH in peptides extracted from the hypothalamus of the indicated mice are shown. Blots are representative of independent experiments with samples from three different mice. Data are means \pm SEM. Significance was calculated by a two-tailed *t* test.

the risk of autism in their offspring (41, 42), and in utero exposure of rodents to VPA is a robust model of autism (42). To investigate the effect of VPA exposure and probiotics treatment on CRH and ACTH cascades in offspring, we conducted a second set of animal experiments including four groups of offspring. Female mice were treated with VPA during pregnancy, and then their offspring mice were split into two groups. One group was treated with NS8 for 1 month (group VNS8^{#2}), and another was not treated (group V^{#2}). In parallel, two groups of offspring from females not treated with VPA with and without probiotics treatment were used as controls (groups NS8^{#2} and C^{#2}, respectively). Analysis of the hypothalamus and pituitary peptidomes for all four groups showed increased abundance of CRH in the hypothalamus of the V^{#2} group compared to the C^{#2} group, but the amount of increase was reduced in the VNS8^{#2} group (Fig. 7A). ACTH in the pituitary followed the same trend (Fig. 7B). Immunoblotting supported the results from the peptidomic analysis (Fig. 7, A and B). These data indicate that in utero VPA exposure influenced the CRH and ACTH signaling cascades, and this could be attenuated by postnatal probiotic treatment. Our results demonstrate that CRH can also be altered by NS8. The other peptides screened by our approach (Fig. 5D) therefore merit further in-depth analysis to elucidate their connection with the probiotics and for the potential for probiotics to affect behavioral or physiological functions regulated by those neuropeptides.

DISCUSSION

Previous studies have revealed that the gut and brain communicate with each other and that probiotics have beneficial effects on the function of the nervous system and host behavior (1, 8). Neuropeptides are a diverse class of signaling molecules that are associated with most

physiological processes. Here, we performed an in-depth analysis on the effect of probiotics administration on the brain peptidome. Our study has shown that the brain peptidome was remodeled in spatiotemporal- and probiotic strain-specific patterns that correlated with changes in the gut microbiome. Our comprehensive brain peptidome dataset illustrates the likely important role of these biomolecules in the gut-brain axis.

Neuropeptides, a major component of total brain peptides, are generated from prohormones (precursor proteins) by a series of enzymatic cleavage steps (43). One prohormone may produce many mature neuropeptides with diverse activities and functions. Although transcriptomic and proteomic approaches allow large-scale analysis of biomolecules, the analytical capability and scale are only accurate at the level of transcripts and prohormones, respectively, instead of the bioactive, mature neuropeptides. In comparison, a peptidomic approach allows direct analysis of the endogenous neuropeptides, which enables the detection of posttranslational modifications to the

starting peptide sequence and more accurately reflects physiological prohormone processing. We established a 1-hour peptidomics approach for accurate and rapid analysis of large sample cohorts, the utility and efficiency of which are demonstrated by the high quality of the benchmark dataset. Previous reports showed that certain physiological and environmental changes, such as circadian (44), time-of-day (45), and high-salt or high-fat diet (46, 47), modulate the production of brain peptides. These variable factors have been minimized in this study, with probiotic administration being the major factor altering brain peptides between the control and the probiotic treatment groups. So far, no large-scale brain proteomics investigations of the gut-brain axis have been published. Chen *et al.* (48) reported that the intestinal microbiome and brain metabolome were associated across life span and established a two-layer strategy to analyze the correlation. In addition to metabolites and neuropeptides, a range of bioactive molecules, such as proteins, RNAs, lipids, and others, are worthy of being investigated for new insights into their regulatory roles in the gut-brain axis.

We observed significant correlation between some species of gut bacteria and brain peptides. The bacteria belonged to Lachnospiraceae and Ruminococcaceae, two dominant bacterial families associated with energy metabolism and body weight regulation (49, 50). Gomez-Arango *et al.* (51) investigated the relationship between gut microbiome and metabolic hormones in overweight and obese pregnant women and found that Lachnospiraceae and Ruminococcaceae are strongly correlated with adipokine. Decreased abundance in the relative representation of both of these bacterial families in the gut microbiome is associated with long-term weight gain, with Ruminococcaceae especially exhibiting a protective effect (52). Colonization of a Lachnospiraceae bacterium in obese mice promoted the development of diabetes (53). Our results indicate that many

neuropeptides are correlated with the two bacterial families, including VIP, orexin-B, NPY, α -MSH, neuromedin-B, and somatostatin-28. Most of these neuropeptides are involved in the regulation of energy homeostasis and food intake (37), and publications implicating food intake and related physiological processes ranked highest in our literature mining for those probiotics-altered neuropeptides. Future investigations should be directed to understand the molecular mechanisms by which gut microbes alter these processes through the modulation of neuropeptides.

Another important finding in our study is that the treatment with heat-killed probiotics caused remarkable change of the peptidome profile in the hippocampus. Thermal-processed and nonviable probiotics are called paraprobiotics (54). These dead probiotics, which contain active components like peptidoglycan fragments and DNA that can modulate immune functions, are suitable for commercial development of therapeutic products because of the advantages of easier storage and longer product shelf life. Ou *et al.* (55) reported that heat-killed lactic acid bacteria enhanced immunomodulatory ability by switching the immune response. In our results, there was no significant change at the level of genus by heat-killed NS8 treatment, and PCoA analysis showed no separation, indicating that heat-killed NS8 did not change the microbiome composition. Overall, our results provide peptidome-level evidence that heat-killed probiotics can affect the gut-brain axis without affecting the composition of the gut microbiome.

In our previous reports, treatment with NS8 improved behavioral and cognitive impairments induced by chronic restraint stress in rats (17), and administration of NS9 restored antibiotics-induced psychological aberrations (28). In this study, we observed that the two probiotics *L. helveticus* NS8 and *L. fermentum* NS9, both belonging to the *Lactobacillus* family, exhibited strain-specific effects for regulation of the brain peptidome. It has been accepted that the mechanisms and actions of probiotics are strain specific, and each strain presents a specific health benefit. Buffington *et al.* (16) reported that *L. reuteri* treatment restored social deficits of mice, but *Lactobacillus johnsonii* had no effect. Wall *et al.* (56) evaluated the administration of *Bifidobacterium breve* strains NCIMB 702258 and DPC 6330, observing altered fatty acid composition in mouse brains. The most significantly altered fatty acids in that study, arachidonic acid and docosahexaenoic acid, play important roles in neurogenesis and neurotransmission. In our study, administration of NS8 and NS9 resulted in distinct changes to the gut microbiome and brain peptidome. Our data reveal the peptide-level signature of strain-specific effects, which might be one of the reasons why different probiotics strains offer diverse beneficial and therapeutic consequences.

Our current study provides strong evidence to support that probiotics can alter the brain peptidome. It has been proposed that probiotics might change the microbiota composition or directly modulate the pathways involved in the conversation between gut and brain, including the host's immune system, vagus nerve, and/or metabolites (12, 39, 57, 58). The former model involves regulation through the microbiota-gut-brain axis, whereas the latter involves direct action through the gut-brain axis. Our results show that probiotics can modulate the brain peptidome through both mechanisms. Live NS8 altered the gut microbiota, but heat-killed NS8 treatment altered the brain peptidome without changing the gut microbiome, demonstrating possible direct action through the gut-brain axis. Several genera of gut bacteria were highly correlated with specific brain peptides, suggesting functional connections. Thus, probiotics administration

might alter the brain peptidome through both the gut-brain axis and the microbiota-gut-brain axis.

There are many gut peptide hormones (59) involved in modulation of the gut-brain axis. Gut microbes increase the proliferation of enteroendocrine L cells that release glucagon-like peptide 1 (GLP-1) and peptide YY (PYY), both of which play appetite-regulatory roles (60). Also, the gut microbes generate short-chain fatty acids that stimulate the secretion of GLP-1 and PYY (61). These peptide hormones enter the circulatory system and affect the brain. Among the brain peptides identified in this study, some of them are also produced in the gut. One example is VIP, which is produced in many organs, including the brain and gut (35), and this peptide in the hypothalamus showed significant correlation with *Anaerotruncus* in our results. The microbes may interact directly with intestinal cells to promote the production of VIP that enters the circulation and disseminates to the brain, or they may indirectly modulate VIP production in the brain. Addressing these possibilities merits further investigation.

In conclusion, our study reveals that oral administration of probiotics can alter the brain peptidome through the gut-brain axis, and the brain peptidome correlated with the composition of the gut microbiome. We provide a dynamic peptidome landscape across different brain regions, treatment times, and strains of probiotics, as well as a paraprobiotics. Overall, these information-rich datasets paint a quantitative picture of brain peptides in relation to gut bacteria as well as related physiological processes and behaviors, demonstrating the power of our 1-hour peptidomics approach to elucidate the molecular mechanisms of the gut-brain axis and highlighting the therapeutic potentials of probiotics.

MATERIALS AND METHODS

Bacteria and animals

The *L. helveticus* NS8 and *L. fermentum* NS9 strains (17, 28) were inoculated into MRS (De Man, Rogosa and Sharpe agar) medium at 37°C for 18 hours each. Then, the bacteria were collected by centrifugation at 3000 rpm for 5 min and washed twice with phosphate-buffered saline (PBS) buffer. The pellet was resuspended in drinking water at a concentration of 10⁹ colony-forming units/ml to feed the animals for probiotic treatment. The heat-killed probiotics were prepared by keeping at 121°C for 30 min.

Two-month-old male specific pathogen-free C57BL/6 J mice (Vital River Laboratories Co. Ltd.) were individually housed during the experiment under standard laboratory conditions (17). A regular diet was supplied with 0.3% salt, 5% fat, 22% protein, and 58% carbohydrates (Vital River Laboratories Co. Ltd). After 2 weeks of accommodation, mice were randomly divided into seven groups for treatment ($n = 12$ each group, details shown in the legend of Fig. 1). Specifically, the NS8 and NS8NS8 groups were fed with probiotics NS8 respectively for 1 and 2 months. The NS9 and NS8h groups were treated with NS9 and heat-killed NS8, respectively. The NS8C group was treated with NS8 in the first month and not treated in the second month. As controls, the C and CC groups were fed with regular water. The mice accessed the probiotics-containing water *ad libitum* over the treatment period as previously reported (16, 17, 62), which was changed daily to minimize dosage variation. The body weight of mice was measured monthly, and no significant change of body weight of mice caused by probiotics treatment was observed. At the end of treatment, the mice were randomly taken out from cages at 9:00 a.m.

to minimize the effect of time difference on brain peptide change (44, 45) and then quickly euthanized for sample collection.

For the prenatal stress experiment (63), the pregnant C57BL/6 J mice at embryonic day 12 (Vital River Laboratories Co. Ltd.) were subcutaneously injected with VPA or PBS (600 mg/kg). Their offspring mice were weaned at postnatal day 21 and divided into four groups (details shown in the legend of Fig. 7). The four offspring groups at postnatal day 35 were respectively treated with water or probiotics for an additional 2 months until euthanized. The animals' care was in accordance with institutional guidelines of National Center for Protein Sciences–Beijing and Institute of Psychology, Chinese Academy of Sciences.

Sample preparation

Mice were anesthetized with isoflurane before being decapitated. Brains were immediately dissected, and the brain region boundaries were carefully checked according to The Mouse Brain Library (www.mbl.org/). The tissues were heated using a microwave oven at 800 W for 9 s (64, 65) and stored at -80°C until further use. For peptide extraction, the tissues were manually homogenized with a glass-glass Dounce grinder. The homogenized samples were combined and centrifuged at 20,000g for 10 min at 4°C to remove the insoluble pellet. This extraction step was repeated three times. Extracts were combined and dried down in a SpeedVac vacuum concentrator. Crude peptide sample was further desalted by C18 ZipTip and resuspended in 5 μl of 0.1% formic acid aqueous solution for LC-MS/MS analysis.

LC-MS/MS analysis

The LC-MS/MS experiments were performed on an Orbitrap Q Exactive HF mass spectrometer (Thermo Fisher Scientific) coupled with an online EASY-nLC 1200 nano-high-performance liquid chromatography (HPLC) system (Thermo Fisher Scientific). The peptide mixtures were separated on a reversed-phase nano-HPLC C18 column [precolumn: 3 μm , 2 cm by 100 μm inner diameter (ID); analytical column: 1.9 μm , 12 cm by 150 μm ID] at a flow rate of 600 nl/min with a 65-min gradient: 3 to 7% solvent B for 1 min, 7 to 12% for 8 min, 12 to 22% for 33 min, 22 to 32% for 10 min, 32 to 55% for 10 min, and 55 to 90% for 3 min (solvent A, water; solvent B, acetonitrile; 0.1% formic acid). The electrospray voltage was 2.2 kV. Peptides were analyzed by data-dependent MS/MS acquisition mode with a resolution of 120,000 at full-scan mode and 15,000 at MS/MS mode. The full scan was processed in the Orbitrap from mass/charge ratio 250 to 1800; the top 20 most intense ions in each scan were automatically selected for higher-energy collisional dissociation (HCD) fragmentation with normalized collision energy of 29% and measured in Orbitrap. Typical mass spectrometric conditions were as follows: Automatic gain control targets were 3×10^6 ions for full scans and 2×10^5 for MS/MS scans; the maximum injection time was 80 ms for full scans and 80 ms for MS/MS scans; and dynamic exclusion was used for 13 s. Each sample was analyzed with one technical replicate because of limited sample volume.

Peptide identification and quantification by PEAKS Studio

Raw data were processed with PEAKS Studio version 8.5 against our purpose-made neuropeptide database (aggregation and filtration of publicly accessible databases: Neuropeptides.nl (36), SwePep (31), Neuropred.com (29), and Neuropedia.com (66)) or a customized UniProt protein database (downloaded on 23 November 2017, encompassing 87,215 protein sequence entries). Mass tolerance for

searches was set to a maximum of 10 parts per million for peptide masses and 0.02 Da for HCD fragment ion masses. Enzyme was set to none. The pyroglutamylation (N-terminal Q, E), oxidation (M), amidation (C terminus), phosphorylation (S, T), and acetylation (K) were set as variable modifications. The identified peptides were filtered by these criteria: (i) false discovery rate $< 1\%$, (ii) identified in ≥ 4 biological replicates, and (iii) containing ≥ 5 amino acids. For peptides with five and six amino acids, further curation was performed by inspecting whether the fragment ions contained a sequence tag of ≥ 3 consecutive b or y ions. The C-terminal amidated peptides without a preceding glycine were considered as false-positive assignments and removed (67). The label-free quantitation based on extracted ion chromatograms was performed using the PEAKS Q module. Only peptides with valid quantitative values of $\geq 70\%$ in at least one group were kept. The sample degradation was examined by inspecting the percentage of basic-cleavage-site-containing peptides (data file S8). The quantitative information was exported as .csv files for further bioinformatics processing.

16S rRNA gene sequencing and analysis

The bacterial genomic DNA was extracted from mouse fecal pellets using the MO BIO PowerSoil Kit. The V3 and V4 regions of the 16S rRNA gene were amplified by polymerase chain reaction (PCR) and sequenced in the Illumina MiSeq 2500 platform. The 2×250 -base pair paired-end protocol was used with individually barcoded universal primers containing adapters for pooling and direct sequencing of PCR products. A quality filter was applied to the resulting merged reads. Reads with Q value of < 25 were discarded. The 16S rRNA gene sequences were clustered into operational taxonomic units (OTUs) at a similarity cutoff value of 97% using the Uclust algorithm. The taxonomies were determined by mapping OTUs to the SILVA database (68). The α diversity and β diversity were generated with the Quantitative Insights Into Microbial Ecology (QIIME) pipeline (69) and calculated on the basis of unweighted UniFrac distance matrices.

Dot blotting

Dot blotting was carried out for orthogonal validation of quantification results from LC-MS. The normalization factor of each sample was calculated according to total ion chromatograph (70) by PEAKS Studio, and the sample loading amount is equal to volume divided by normalization factors. The peptide samples were spotted directly onto nitrocellulose membranes, which were then blocked with 5% nonfat dry milk in tris-buffered saline (TBS) with 0.05% Tween 20. The membrane was incubated in primary antibodies overnight at 4°C . The rabbit polyclonal anti-CRH (Abcam, ab8901) and anti-ACTH (Abcam, ab74976) antibodies were diluted to 1:500. After washing three times for 5 min with 0.05% TBST, the membranes were incubated with peroxidase-conjugated goat anti-rabbit secondary antibody (ZSGB-Bio, 2301) for 1 hour at room temperature. Reactivity was visualized using enhanced chemiluminescence substrate (CWBio, CW0048M). Each experiment was repeated three times.

Data analysis

R scripts were used for all data analyses and visualizations in this study. For peptidomics data analysis, peptides with valid quantitative values (PEAKS quality score > 0.2) were filtered for downstream analysis. The raw abundance values were \log_2 -transformed. Missing values were then replaced with a constant value of zero. Differentially expressed peptides between groups were identified by a two-tailed

t test with unequal variances. The criterion to identify significant differences was $P < 0.05$. Expression patterns of peptides in C, NS8, and NS8h groups were further analyzed by a hierarchical clustering method with Euclidean distance and average linkage in R.

Amino acid sequence logo plots were drawn by IceLogo 1.2, which was scaled on the amino acid frequencies found in *Mus musculus*.

Neuropeptides were classified by the families of the genes encoding them, and there were 25 gene families, of which 17 were classified by the neuropeptide database [www.neuropeptides.nl (36)], and the remaining 8 named by corresponding precursors.

To identify significant changes in bacteria abundance, we investigated the genus levels of bacteria. Different expression of genus between C group and NS8 group were identified by a two-tailed *t* test with unequal variances. *P* values of <0.05 were considered significant. To uncover the links between brain peptidome and gut microbiome, Spearman's correlation coefficients (*r* values) were calculated between peptides and the four significantly altered bacteria genera. Those with *r* values > 0.5 or < -0.5 were considered significant.

Literature mining

A neuropeptide text mining algorithm was implemented in R scripts (listed in data file S9). Detailed procedure is as follows.

1) PubMed entries with Medical Subject Headings terms containing the words mouse, neuropeptide, and hypothalamus were selected as corpus. Each entry in the corpus contains PubMed Identifier, article title, and abstract. Abstracts were segmented into sentences by R package natural language processing (NLP).

2) To obtain behavior-related sentences, we compiled a small behavioral dictionary (data file S9) used for screening sentences with the matching tokens. The resulting sentences were further extracted and compiled into a target statement library. The R package coreNLP split sentences in the target statement library to words, performed part-of-speech tagging, and extracted sentence syntactic structure and grammatical relations.

3) The sentences containing a list of target verbs (data file S9) and conforming the grammatical structure of (neuropeptide) subject-verb-object (behavior) were extracted. Target verbs can indicate how neuropeptides regulate behavior and in what way.

4) Last, the sentences were grouped into six behavioral categories: anxiety and depression, food intake, sleep/awake and circadian, social and reproductive behaviors, nociception, and cognition. The number of publications in each group was counted.

SUPPLEMENTARY MATERIALS

stke.sciencemag.org/cgi/content/full/13/642/eabb0443/DC1

Fig. S1. Data quality of the 1-hour peptidomics approach in analysis of hypothalamus peptides.

Fig. S2. Quality control of the quantitative peptidomics.

Fig. S3. Gut microbiome compositions resulting from 16S rRNA analysis.

Fig. S4. Histogram illustrates the total quantifiable and significantly altered hypothalamus peptides (unique sequences) of the CC/C dataset resulting from 1-month development of mice.

Fig. S5. Hierarchical clustering shows the brain peptide change in hypothalamus among the C, NS8, and NS9 groups.

Table S1. Neuropeptide families.

Data file S1. Identified peptides from four brain regions (corresponding to Fig. 2A) (Excel file).

Data file S2. Detailed information of peptides shown in Fig. 2D (Excel file).

Data file S3. Detailed information of correlation analysis shown in Fig. 3C (Excel file).

Data file S4. Detailed information of clustering analysis shown in Fig. 3E (Excel file).

Data file S5. Detailed information of peptidome shown in Fig. 4A (Excel file).

Data file S6. Detailed information of peptidome shown in Fig. 4D (Excel file).

Data file S7. Detailed information of peptidome shown in Fig. 5, D and F (Excel file).

Data file S8. Percentage of basic-cleavage-site-containing peptides (Excel file).

Data file S9. Detailed information of MINlbar script (Excel file).

[View/request a protocol for this paper from Bio-protocol.](#)

REFERENCES AND NOTES

- G. Sharon, T. R. Sampson, D. H. Geschwind, S. K. Mazmanian, The central nervous system and the gut microbiome. *Cell* **167**, 915–932 (2016).
- H. E. Vuong, J. M. Yano, T. C. Fung, E. Y. Hsiao, The microbiome and host behavior. *Annu. Rev. Neurosci.* **40**, 21–49 (2017).
- R. Diaz Heijtz, S. Wang, F. Anuar, Y. Qian, B. Bjorkholm, A. Samuelsson, M. L. Hibberd, H. Forsberg, S. Pettersson, Normal gut microbiota modulates brain development and behavior. *Proc. Natl. Acad. Sci. U.S.A.* **108**, 3047–3052 (2011).
- C. de la Fuente-Nunez, B. T. Meneguetti, O. L. Franco, T. K. Lu, Neuroimmunology: How microbes influence the brain. *ACS Chem. Neurosci.* **9**, 141–150 (2018).
- H. E. Vuong, E. Y. Hsiao, Emerging roles for the gut microbiome in autism spectrum disorder. *Biol. Psychiatry* **81**, 411–423 (2017).
- T. Harach, N. Marungu, N. Duthilleul, V. Cheatham, K. D. Mc Coy, G. Frisoni, J. J. Neher, F. Fak, M. Jucker, T. Lasser, T. Bolmont, Reduction of Abeta amyloid pathology in APPPS1 transgenic mice in the absence of gut microbiota. *Sci. Rep.* **7**, 41802 (2017).
- A. Parashar, M. Udayabanu, Gut microbiota: Implications in Parkinson's disease. *Parkinsonism Relat. Disord.* **38**, 1–7 (2017).
- J. A. Foster, K. A. McVey Neufeld, Gut-brain axis: How the microbiome influences anxiety and depression. *Trends Neurosci.* **36**, 305–312 (2013).
- S. Liang, X. Wu, X. Hu, T. Wang, F. Jin, Recognizing depression from the microbiota–gut–brain axis. *Int. J. Mol. Sci.* **19**, 1592 (2018).
- K. A. Neufeld, N. Kang, J. Bienenstock, J. A. Foster, Effects of intestinal microbiota on anxiety-like behavior. *Commun. Integr. Biol.* **4**, 492–494 (2011).
- M. Messaoudi, R. Lalonde, N. Violle, H. Javelot, D. Desor, A. Nejdj, J. F. Bisson, C. Rougeot, M. Pichelin, M. Cazaubiel, J. M. Cazaubiel, Assessment of psychotropic-like properties of a probiotic formulation (*Lactobacillus helveticus* R0052 and *Bifidobacterium longum* R0175) in rats and human subjects. *Br. J. Nutr.* **105**, 755–764 (2011).
- X. Liu, S. Cao, X. Zhang, Modulation of gut microbiota-brain axis by probiotics, prebiotics, and diet. *J. Agric. Food Chem.* **63**, 7885–7895 (2015).
- J. A. Bravo, P. Forsythe, M. V. Chew, E. Escaravage, H. M. Savignac, T. G. Dinan, J. Bienenstock, J. F. Cryan, Ingestion of *Lactobacillus* strain regulates emotional behavior and central GABA receptor expression in a mouse via the vagus nerve. *Proc. Natl. Acad. Sci. U.S.A.* **108**, 16050–16055 (2011).
- K. A. McVey Neufeld, S. Kay, J. Bienenstock, Mouse strain affects behavioral and neuroendocrine stress responses following administration of probiotic *Lactobacillus rhamnosus* JB-1 or traditional antidepressant fluoxetine. *Front. Neurosci.* **12**, 294 (2018).
- E. Y. Hsiao, S. W. McBride, S. Hsien, G. Sharon, E. R. Hyde, T. McCue, J. A. Codelli, J. Chow, S. E. Reisman, J. F. Petrosino, P. H. Patterson, S. K. Mazmanian, Microbiota modulate behavioral and physiological abnormalities associated with neurodevelopmental disorders. *Cell* **155**, 1451–1463 (2013).
- S. A. Buffington, G. V. Di Prisco, T. A. Auchtung, N. J. Ajami, J. F. Petrosino, M. Costa-Mattioli, Microbial reconstitution reverses maternal diet-induced social and synaptic deficits in offspring. *Cell* **165**, 1762–1775 (2016).
- S. Liang, T. Wang, X. Hu, J. Luo, W. Li, X. Wu, Y. Duan, F. Jin, Administration of *Lactobacillus helveticus* NS8 improves behavioral, cognitive, and biochemical aberrations caused by chronic restraint stress. *Neuroscience* **310**, 561–577 (2015).
- L. D. Fricker, J. Lim, H. Pan, F.-Y. Che, Peptidomics: Identification and quantification of endogenous peptides in neuroendocrine tissues. *Mass Spectrom. Rev.* **25**, 327–344 (2006).
- A. N. van den Pol, Neuropeptide transmission in brain circuits. *Neuron* **76**, 98–115 (2012).
- L. Li, J. V. Sweedler, Peptides in the brain: Mass spectrometry-based measurement approaches and challenges. *Annu. Rev. Anal. Chem.* **1**, 451–483 (2008).
- H. Ye, J. Wang, Z. Tian, F. Ma, J. Dowell, Q. Bremer, G. Lu, B. Baldo, L. Li, Quantitative mass spectrometry reveals food intake-induced neuropeptide level changes in rat brain: Functional assessment of selected neuropeptides as feeding regulators. *Mol. Cell. Proteomics* **16**, 1922–1937 (2017).
- F. Petruzzello, S. Falasca, P. E. Andren, G. Rainer, X. Zhang, Chronic nicotine treatment impacts the regulation of opioid and non-opioid peptides in the rat dorsal striatum. *Mol. Cell. Proteomics* **12**, 1553–1562 (2013).
- C. Jia, L. Hui, W. Cao, C. B. Lietz, X. Jiang, R. Chen, A. D. Catherman, P. M. Thomas, Y. Ge, N. L. Kelleher, L. Li, High-definition de novo sequencing of crustacean hyperglycemic hormone (CHH)-family neuropeptides. *Mol. Cell. Proteomics* **11**, 1951–1964 (2012).
- C. Jia, C. B. Lietz, H. Ye, L. Hui, Q. Yu, S. Yoo, L. Li, A multi-scale strategy for discovery of novel endogenous neuropeptides in the crustacean nervous system. *J. Proteomics* **91**, 1–12 (2013).

authors have approved the final manuscript. **Competing interests:** The authors declare that they have no competing interests. **Data and materials availability:** The MS proteomics data have been deposited to the ProteomeXchange Consortium (<http://proteomecentral.proteomexchange.org>) through the iProX partner repository (71) with the dataset identifier PXD015323. The 16S rRNA sequence data have been deposited in the National Center for Biotechnology Information (NCBI) database with accession code PRJNA612927. All other data needed to evaluate the conclusions in the paper are present in the paper or the Supplementary Materials.

Submitted 25 January 2020

Accepted 10 June 2020

Published 28 July 2020

10.1126/scisignal.abb0443

Citation: P. Zhang, X. Wu, S. Liang, X. Shao, Q. Wang, R. Chen, W. Zhu, C. Shao, F. Jin, C. Jia, A dynamic mouse peptidome landscape reveals probiotic modulation of the gut-brain axis. *Sci. Signal.* **13**, eabb0443 (2020).

A dynamic mouse peptidome landscape reveals probiotic modulation of the gut-brain axis

Pei Zhang, Xiaoli Wu, Shan Liang, Xianfeng Shao, Qianqian Wang, Ruibing Chen, Weimin Zhu, Chen Shao, Feng Jin and Chenxi Jia

Sci. Signal. **13** (642), eabb0443.
DOI: 10.1126/scisignal.abb0443

The brain on probiotics

Besides being a key player in the regulation of host metabolism and immunity, the gut microbiome also plays an important role in the gut-brain axis, a system of bidirectional communication between the central and enteric nervous systems. Zhang *et al.* analyzed the brain peptidomes and gut microbiomes of mice fed two different species of probiotics. Probiotic treatment altered the abundances of many neuropeptides in a manner that correlated with changes in the composition of the gut microbiome, varied by brain region, and depended on the probiotic species, whether the probiotic was live or heat-killed, and the duration of treatment. These omics datasets are a foundation for future studies of the mechanistic links between the gut microbiota and cognitive, behavioral, and physiological processes controlled by neuropeptides.

ARTICLE TOOLS

<http://stke.sciencemag.org/content/13/642/eabb0443>

SUPPLEMENTARY MATERIALS

<http://stke.sciencemag.org/content/suppl/2020/07/24/13.642.eabb0443.DC1>

RELATED CONTENT

<http://stke.sciencemag.org/content/sigtrans/11/520/eaan6480.full>
<http://stke.sciencemag.org/content/sigtrans/12/588/eaaw3159.full>
<http://science.sciencemag.org/content/sci/366/6465/eaar2016.full>
<http://science.sciencemag.org/content/sci/365/6460/1405.full>
<http://advances.sciencemag.org/content/advances/5/2/eaau8317.full>
<http://advances.sciencemag.org/content/advances/6/11/eaax6328.full>
<http://stm.sciencemag.org/content/scitransmed/11/520/eaaw3521.full>
<http://immunology.sciencemag.org/content/immunology/3/20/eaao1603.full>

REFERENCES

This article cites 70 articles, 11 of which you can access for free
<http://stke.sciencemag.org/content/13/642/eabb0443#BIBL>

PERMISSIONS

<http://www.sciencemag.org/help/reprints-and-permissions>

Use of this article is subject to the [Terms of Service](#)

Science Signaling (ISSN 1937-9145) is published by the American Association for the Advancement of Science, 1200 New York Avenue NW, Washington, DC 20005. The title *Science Signaling* is a registered trademark of AAAS.

Copyright © 2020 The Authors, some rights reserved; exclusive licensee American Association for the Advancement of Science. No claim to original U.S. Government Works